Conformationally Restricted Competitive Antagonists of Human/Rat Corticotropin-Releasing Factor‡

Antonio Miranda, Steven C. Koerber, Jozsef Gulyas, Sabine L. Lahrichi, A. Grey Craig, Anne Corrigan, Arnold Hagler,† Catherine Rivier, Wylie Vale, and Jean Rivier*

The Clayton Foundation Laboratories for Peptide Biology, The Salk Institute for Biological Studies, 10010 North Torrey Pines Road, La Jolla, California 92037

Received March 11, 1993•

Corticotropin releasing factor (CRF) is a 41-peptide amide which stimulates the release of ACTH (Vale et al. *Science* **1981**, *213*, 1394). CRF has been postulated to assume an α-helical conformation upon binding to its pituitary receptor (Hernandez et al. *J. Med. Chem.* **1993**, *36*, 2860). We have exploited this hypothesis in the design of a limited series of cyclic analogues and have taken into consideration the effects of side-chain deletion (Alanine scan, Kornreich et al. *J. Med. Chem.* **1992**, *35*, 1870) as well as of changes in chirality (Rivier et al. *J. Med. Chem.* **1993**, *36*, 2851), with the rationale that side chains necessary for binding could also be replaced by side-chain bridges. In particular, we have used computer modeling to predict likely side chain bridging opportunities and evaluated the effects of such replacements by correlating biological results with those derived from CD spectroscopy. We have synthesized 38 monocyclic peptide amides, competitive antagonists of human/rat CRF, using solid-phase methodology on MBHA resin. After purification by preparative RP-HPLC, the peptides were analyzed by RP-HPLC and capillary zone electrophoresis and characterized by mass spectroscopy and amino acid analysis. CRF antagonists were tested for their ability to interfere with CRF-induced release of ACTH by rat anterior pituitary cells. In most cases, one of the bridge heads was located at a position where substitution by a D-residue was tolerated (i.e., positions 12 and 20). It has become clear that careful optimization of bridge length and chirality is critical. This is best exemplified by the fact that out of the 38 analogues that were synthesized and tested, only two, {cyclo(20–23)[DPhe^{12},Glu^{20},Lys^{23},Nle^{21,38}]h/rCRF$_{12-41}$ and cyclo-(20–23)[DPhe^{12},Glu^{20},Orn^{23},Nle^{21,38}]h/rCRF$_{12-41}$}, were found to be more potent (3 and 2 times, respectively) than [DPhe^{12},Nle^{21,38}]h/rCRF$_{12-41}$, the parent compound. Six analogues belonging to two different families were found to be half as potent as the standard, 18 had 2–20% of the potency of the standard, and the others were significantly less potent. CD results of all analogues in 50% TFE (a concentration of TFE that induced nearly maximum helicity of [DPhe^{12},Nle^{21,38}]h/rCRF$_{12-41}$) suggest that while helicity may be an important factor for CRF analogue recognition, little correlation is found between percent helicity as determined by spectral deconvolution and biological activity *in vitro*.

Introduction

Corticotropin releasing factor (CRF) was originally characterized from ovine hypothalamus by Vale et al. in 1981.[1] Since then, homologous CRF sequences from several other mammalian species have been either isolated and characterized[2–6] or cloned.[7–10] The primary sequence of human/rat CRF is Ser-Glu-Glu-Pro-Pro-Ile-Ser-Leu-Asp-Leu^{10}-Thr-Phe-His-Leu-Leu-Arg-Glu-Val-Leu-Glu^{20}-Met-Ala-Arg-Ala-Glu-Gln-Leu-Ala-Gln-Gln^{30}-Ala-His-Ser-Asn-Arg-Lys-Leu-Met-Glu-Ile^{40}-Ile-NH_2. Also, non-mammalian peptides with homologous sequences have been isolated and characterized (sauvagine,[11,12] the urotensins,[13,14] and two diuretic peptides isolated from tobacco hornworm, *Manduca sexta*[15,16]) or cloned.[17] These peptides were synthesized and tested for their ability to release ACTH and were all found to be equipotent in the *in vitro* assay reported here.[18] Members of the CRF family have been found to have many additional activities resulting in the alteration of the cardiovascular system, behavior, reproduction, gastrointestinal secretion, intestinal motility, and transit.[19–21] These peptides are also present in a large number of tissues.[22,23] Most importantly, CRF is involved in a wide spectrum of CNS-mediated effects which suggest that this peptide plays an important role within the brain, especially during stress.[19–21] Because of this diversity of action, potent competitive antagonists of CRF have been extremely useful in the study of the physiologic and pathophysiologic role of CRF.[24–26] Ultimately, it is hoped that such analogues will play a major role in the management of some stress-related states.[27–32] In view of studies suggesting that each member of the CRF family possessed

† Current address: Biosym Technologies, Inc., 9685 Scranton Rd., San Diego, CA 92121-2777.

‡ Abbreviations: The abbreviations for the amino acids are in accord with the recommendations of the IUPAC–IUB Joint Commission on Biochemical nomenclature (*Eur. J. Biochem.* **1984**, *138*, 9–37). The symbols represent the L-isomer except when indicated otherwise. In addition: AcOH, acetic acid; ACTH, adrenocorticotropin hormone; Aib, aminoisobutyric acid; Boc, *tert*-butoxycarbonyl; BOP, (benzotriazol-1-yloxy)-tris(dimethylamino)phosphonium hexafluorophosphate; Bzl, benzyl ester; C_{18}, octadecyl; CD, circular dichroism; CH_3CN, acetonitrile; CNS, central nervous system; CRF, corticotropin releasing factor; CZE, capillary zone electrophoresis; Dbu, 2,4-diaminobutyric acid; DCHA, dicyclohexylamine; DCM, dichloromethane; DIC, 1,3-diisopropylcarbodiimide; DIEA, diisopropylethylamine; DMF, dimethylformamide; Dpr, 2,3-diaminopropionic acid; EDT, ethanedithiol; Fmoc, 9*H*-fluorenylmethoxycarbonyl; HF, hydrogen fluoride; HOBt, 1-hydroxybenzotriazole; HPLC, high-performance liquid chromatography; h/rCRF, human/ratCRF; i-PrOH, 2-propanol; LSIMS, liquid secondary ion mass spectrometry; MBHA, 4-methylbenzhydrylamine; MeOH, methanol; Nle, norleucine; NMP, *N*-methylpyrrolidone; OcHx, cyclohexyl ester; OFm, fluorenylmethyl ester; oCRF, ovine CRF; RPHPLC, reversed-phase high-performance liquid chromatography; RT, retention time; SAR, structure–activity relationship; SEM, standard error of the mean; TEA, triethylamine; TEAP 2.25, triethylammonium phosphate with pH adjusted to 2.25; TFA, trifluoroacetic acid; TFE, 2,2,2-trifluoroethanol; Tos, *p*-toluenesulfonyl; 2ClZ, 2-chlorobenzyloxycarbonyl; CNS, central nervous system.

• Abstract published in *Advance ACS Abstracts*, April 15, 1994.

0022-2623/94/1837-1450$04.50/0

considerable amphiphilic α-helical stretches,[12,33,34] Rivier et al.[24] built a chimeric molecule which was found to be 3 times as potent as CRF. On the basis of this structure, an antagonist, α-helical-CRF_{9-41} (Asp-Leu-Thr-Phe-His-Leu-Leu-Arg-Glu-Met-Leu-Glu-Met-Ala-Lys-Ala-Glu-Gln-Glu-Ala-Glu-Gln-Ala-Ala-Leu-Asn-Arg-Leu-Leu-Leu-Glu-Glu-Ala-NH_2) was designed.[24] This analogue proved important by showing marked differences in its ability to antagonize the actions of CRF in three *in vivo* bioassay systems. This suggested the existence of different CRF receptor subtypes.[35] SAR studies in our laboratories led to the observation that the introduction of Nle residues at positions 21 and 38 generated analogues that were significantly more potent than the α-helical-CRF_{9-41}.[36] One such antagonist, [DPhe[12],Nle[21,38]]h/$rCRF_{12-41}$, presently used as our standard, is ca. 18 times more potent than α-helical-CRF_{9-41} in inhibiting the release of ACTH by rat pituitary cells in culture.[37]

A complementary approach to understanding the mechanism of CRF/receptor interaction would be to investigate the effect of structural constraints on activity and biopotency. Three specific issues should be addressed: (i) the positions in a sequence where bridgeheads should be introduced, (ii) the chirality of the bridgeheads, and (iii) the length of the bridge. Because physicochemical evidence (CD), NMR,[38] and SAR studies (Nα-methylation and Cα-methylation[39]) suggest that CRF assumes an α-helical structure in solution or when interacting with its receptor, we have searched for structural constraints that would unequivocally lock such structural motifs into the overall structure. Side chain–side chain bridging (either through disulfide or lactam bridges) offers such an opportunity. Whereas Felix et al.[40] took advantage of putative salt bridges as the rationale for the location of bridgeheads in GRF, we independently introduced bridgeheads in GRF at positions where (at least for one of the bridgeheads) introduction of a D-residue increased potency.[41] Here, we report: (a) the hypotheses that led to the synthesis of 38 constrained analogues of human/ratCRF_{12-41}, (b) their relative biological potencies in inhibiting ACTH release from pituitary cells in culture, and (c) the conclusions that we can draw as to the nature of CRF's bioactive conformation based on CD studies and molecular modeling. Preliminary results were presented at the 12th American Peptide Symposium.[37]

Results

Peptides Synthesis, Purification, and Characterization. Stepwise synthesis of the cyclic peptides was carried out using manual solid-phase methodology on methylbenzhydrylamine-resin (MBHA-resin)[42] with *tert*-butoxycarbonyl (Boc)-protected amino acids and with 1,3-diisopropylcarbodiimide (DIC) as coupling agent. OFm/Fmoc protecting groups were used for the orthogonal protection of the amino acid side chains used as bridge heads. Recouplings and cyclization on the resin were done using (benzotriazol-1-yloxy)tris(dimethylamino)phosphonium hexafluorophosphate (BOP)[43] in the presence of excess diisopropylethylamine (DIEA). Peptides containing cysteine residues were air-oxidized after HF deprotection and cleavage from the resin. Lactam formation for the other cyclic analogues used essentially two strategies. In the first strategy (**5–8, 13–15, 18, 19, 22–30, 32–35, 38**) cyclization was effected upon complete synthesis of the peptide. In the second strategy (**9–12, 16, 17, 20, 31, 36–37**) cyclization was achieved immediately after the introduction of the last element of the bridge and prior to completion of the whole sequence. After completion of the synthesis, the protected, cyclized peptide was cleaved from the resin in liquid HF in the presence of a scavenger, extracted, and lyophilized. It is interesting to note that the first strategy seems to have generated purer compounds resulting in higher yields. The alternate reasoning behind using these two strategies was that a more flexible peptide (i.e., shorter in the case of **9–12, 16, 17, 20, 31, 36–37**) would be more likely to cyclize easily or cyclization would be favored under conditions whereby the peptide would assume a more rigid conformation that would favor proximity of those side chains to be cyclized. Because of the fact that the location of the bridges was not equivalent or identical in these two sets of experiments, it is difficult to assess whether one or the other strategy is clearly better than the other. A source of structure ambiguity was pointed out to us by one of the referees who suggested the possibility of β-aspartyl linkage for compounds **33–38** as a result of activation of the β-carboxyl of the Asp residue at position 20 which may proceed through an aspartimide intermediate. At this point two products may be obtained (the desired peptide and the corresponding β-aspartyl derivative) with their ratio depending on steric as well as electrophilic considerations. The point was particularly well taken in view of our prior observations (unpublished results in collaboration with L. Gierasch and J. Rizo) that β-aspartyl peptides readily formed during the synthesis of constrained GnRH analogues as demonstrated by NMR (manuscript in preparation). In the case of GnRH analogues, however, this side reaction was never prevalent, although 50:50 mixes of the desired product and its isomer could be seen in a few instances. In all GnRH analogues, the two isomers were readily separable by RP-HPLC. Analogues **33–38** were submitted to 14 Edman cycles in order to exclude this possibility. Results clearly indicated that we had isolated the desired peptides. Because of the complexity of the crude mixes, it is impossible to conclude whether this side reaction did or did not occur to any significant level in any of the cases presented here. The fact that this reaction was very significant in dicyclic but not in monocyclic GnRH analogues, whereby the Asp containing cycle was formed last, suggests that the supplemental constraints were responsible for that undesired reaction. Crude peptides were purified by preparative reverse-phase HPLC (RP-HPLC) and obtained as the TFA salts. Compounds were subjected to several HPLC purification steps using different solvent systems.[44] Final preparations of the analogues (yields ranged from 3 to 8% of theory based on resin substitution) were analyzed for purity using RP-HPLC and CZE (purity as shown in Table 1) and characterized using optical rotation, mass spectrometry (all in Table 1), and amino acid analysis (not shown). Noteworthy was the observation that in contradistinction with what had been observed with the introduction of a D-amino acid,[45] the optical rotations of the peptides were significantly influenced by the introduction of structural constraints (internal bridges).

Circular Dichroism Spectra. The CD spectrum of the standard, [DPhe[12],Nle[21,38]]h/$rCRF_{12-41}$, was investigated as a function of the concentration of TFE. As shown in Figure 1, even in the absence of TFE this peptide assumes a partially helical structure (20%) as judged by spectral deconvolution using the method of Yang et al.[46] The theoretical helical content at varying concentrations

Table 1. Percent Purity Determined by HPLC, Isocratic Retention Times, Capillary Zone Electrophoresis, Specific Rotations, Mass Spectrometry Data, and Relative Potency for the CRF Cyclic Antagonists

no.	compound	HPLC (%)[a]	iso RT at % CH_3CN[b]	CZE (%)[c]	$[\alpha]^{25}_D$ (deg)[d]	calcd mass (Da)[e]	obsd (m/z)[e]	relative potency in vitro antagonist[f]	IA[g]
1	cyclo(12-15)[Cys^{12},Cys^{15},Nle^{21,38}]h/rCRF$_{12-41}$	98	3.8 at 35.4	99	-16	3481.86	3481.4	0.015 (0.008-0.026)	5
2	cyclo(12-15)[Cys^{12},DCys^{15},Nle^{21,38}]h/rCRF$_{12-41}$	99	3.7 at 31.8	97	-8	3481.86	3481.4	0.003 (0.001-0.005)	9
3	cyclo(12-15)[DCys^{12},DCys^{15},Nle^{21,38}]h/rCRF$_{12-41}$	99	4.0 at 31.8	99	-38	3481.86	3482.0	0.025 (0.009-0.063)	ND
4	cyclo(12-15)[DCys^{12},Cys^{15},Nle^{21,38}]h/rCRF$_{12-41}$	98	4.5 at 33.0	98	-24	3481.86	3481.6	0.006 (0.002-0.014)	ND
5	cyclo(12-15)[DGlu^{12},Lys^{15},Nle^{21,38}]h/rCRF$_{12-41}$	95	3.1 at 31.8	99	-52	3516.97	3517.1	0.006 (0.002-0.014)	10
6	cyclo(12-15)[DGlu^{12},Lys^{16},Nle^{21,38}]h/rCRF$_{12-41}$	98	3.6 at 36.6	98	-24	3473.97	3473.9	0.16 (0.08-0.32)	8
7	cyclo(15-20)[DPhe^{12},Lys^{15},Glu^{20},Nle^{21,38}]h/rCRF$_{12-41}$	98	3.7 at 30.0	99	-66	3535.01	3535.3	<0.001	4
8	cyclo(16-20)[DPhe^{12},Lys^{16},Glu^{20},Nle^{21,38}]h/rCRF$_{12-41}$	95	4.6 at 36.6	97	-53	3491.98	3491.9	0.4 (0.2-0.9)	18
9	cyclo(16-20)[DPhe^{12},Lys^{16},Asp^{20},Nle^{21,38}]h/rCRF$_{12-41}$	95	4.2 at 37.2	95	-38	3477.98	3478.1	0.18 (0.075-0.39)	21
10	cyclo(16-20)[DPhe^{12},Orn^{16},Glu^{20},Nle^{21,38}]h/rCRF$_{12-41}$	95	6.1 at 34.3	96	-65	3477.98	3477.30	0.16 (0.07-0.33)	11
11	cyclo(16-20)[DPhe^{12},Dbu^{16},Glu^{20},Nle^{21,38}]h/rCRF$_{12-41}$	90	4.7 at 33.6	93	-69	3463.97	3463.85	0.021 (0.006-0.055)	4
12	cyclo(16-20)[DPhe^{12},Orn^{16},Asp^{20},Nle^{21,38}]h/rCRF$_{12-41}$	91	3.7 at 33.0	91	-65	3463.97	3463.92	0.001 (0.000-0.004)	2
13	cyclo(16-20)[DPhe^{12},DLys^{16},Glu^{20},Nle^{21,38}]h/rCRF$_{12-41}$	95	4.4 at 34.2	95	-30‡	3491.98	3492.2	0.08 (0.03-0.17)	4
14	cyclo(16-20)[DPhe^{12},DLys^{16},DGlu^{20},Nle^{21,38}]h/rCRF$_{12-41}$	99#	3.2 at 36.0	99	-11‡	3492.00	3491.9	0.2 (0.1-0.4)	5
15	cyclo(16-20)[DPhe^{12},Lys^{16},DGlu^{20},Nle^{21,38}]h/rCRF$_{12-41}$	99#	3.9 at 36.6	99	-21‡	3492.00	3491.7	0.4 (0.2-0.8)	6
16	cyclo(16-20)[DPhe^{12},Lys^{16},DAsp^{20},Nle^{21,38}]h/rCRF$_{12-41}$	100	3.5 at 37.8	99	-41	3477.98	3478.0	0.06 (0.03-0.13)	7
17	cyclo(16-20)[DPhe^{12},Orn^{16},DAsp^{20},Nle^{21,38}]h/rCRF$_{12-41}$	99	4.0 at 34.2	99	-42	3463.97	3464.1	0.006 (0.001-0.019)	
18	cyclo(17-20)[DPhe^{12},Lys^{17},Glu^{20},Nle^{21,38}]h/rCRF$_{12-41}$	95	4.0 at 31.8	99	-55	3519.06	3519.2	0.02 (0.01-0.03)	3
19	cyclo(17-20)[DPhe^{12},Lys^{17},DGlu^{20},Nle^{21,38}]h/rCRF$_{12-41}$	98#	3.8 at 39.0	99	-38‡	3521.20*	3521.3*	<0.001	23
20	cyclo(17-20)[DPhe^{12},Dbu^{17},Asp^{20},Nle^{21,38}]h/rCRF$_{12-41}$	95	3.0 at 32.3	94	-53	3477.01	3477.0	0.005 (0.001-0.013)	9
21	cyclo(17-20)[DPhe^{12},Cys^{17},Cys^{20},Nle^{21,38}]h/rCRF$_{12-41}$	98	3.9 at 30.0	99	-27‡	3483.93	3484.1	0.008 (0.003-0.02)	15
22	cyclo(20-25)[DPhe^{12},DGlu^{20},Lys^{25},Nle^{21,38}]h/rCRF$_{12-41}$	99	4.3 at 38.4	99	-46	3519.06	3519.0	0.05 (0.02-0.1)	25
23	cyclo(20-24)[DPhe^{12},DGlu^{20},Lys^{24},Nle^{21,38}]h/rCRF$_{12-41}$	96	4.6 at 36.0	99	-51	3577.06	3577.1	0.2 (0.1-0.5)	18
24	cyclo(20-23)[DPhe^{12},DGlu^{20},Lys^{23},Nle^{21,38}]h/rCRF$_{12-41}$	98	3.6 at 36.0	99	-41	3492.00	3492.0	0.5 (0.3-0.9)	23
25	cyclo(20-23)[DPhe^{12},Glu^{20},Lys^{23},Nle^{21,38}]h/rCRF$_{12-41}$	98	4.2 at 36.6	98	-49‡	3492.00	3491.7	2.9 (1.3-6.7)	11
26	cyclo(20-23)[DPhe^{12},DGlu^{20},DLys^{23},Nle^{21,38}]h/rCRF$_{12-41}$	98	3.6 at 34.8	99	-65	3492.00	3491.8	0.4 (0.2-0.9)	8
27	cyclo(20-23)[DPhe^{12},Glu^{20},DLys^{23},Nle^{21,38}]h/rCRF$_{12-41}$	98#	3.6 at 40.8	97	-64‡	3492.00	3491.9	0.02 (0.01-0.04)	0
28	cyclo(20-23)[DPhe^{12},Lys^{20},Glu^{23},Nle^{21,38}]h/rCRF$_{12-41}$	98#	3.9 at 33.6	99	-50‡	3492.00	3491.9	0.12 (0.06-0.25)	6
29	cyclo(20-23)[DPhe^{12},DLys^{20},Glu^{23},Nle^{21,38}]h/rCRF$_{12-41}$	99#	3.4 at 35.4	99	-40‡	3492.00	3491.9	0.12 (0.07-0.22)	1
30	cyclo(20-23)[DPhe^{12},DGlu^{20},Orn^{23},Nle^{21,38}]h/rCRF$_{12-41}$	95	3.3 at 34.8	99	-65	3477.98	3478.1	0.2 (0.1-0.3)	1
31	cyclo(20-23)[DPhe^{12},DGlu^{20},Dpr^{23},Nle^{21,38}]h/rCRF$_{12-41}$	98	4.0 at 34.8	98	-66	3449.95	3450.0	0.25 (0.14-0.46)	1
32	cyclo(20-23)[DPhe^{12},Glu^{20},Orn^{23},Nle^{21,38}]h/rCRF$_{12-41}$	98	3.0 at 35.4	98	-67	3477.98	3478.1	2.0 (1.2-3.5)	10
33	cyclo(20-23)[DPhe^{12},Asp^{20},Lys^{23},Nle^{21,38}]h/rCRF$_{12-41}$	97#	4.7 at 39.0	98	-66	3480.10*	3480.1*	<0.001	10
34	cyclo(20-23)[DPhe^{12},DAsp^{20},Lys^{23},Nle^{21,38}]h/rCRF$_{12-41}$	95	3.0 at 39.0	97	-51	3480.10*	3479.9*	0.022 (0.003-0.07)	13
35	cyclo(20-23)[DPhe^{12},DAsp^{20},Orn^{23},Nle^{21,38}]h/rCRF$_{12-41}$	98#	3.3 at 34.2	98	-58	3463.97	3464.0	0.4 (0.2-0.7)	1
36	cyclo(20-23)[DPhe^{12},DAsp^{20},Dbu^{23},Nle^{21,38}]h/rCRF$_{12-41}$	99	3.5 at 34.8	99	-66	3445.95	3450.1	0.4 (0.17-0.93)	3
37	cyclo(20-23)[DPhe^{12},DAsp^{20},Dpr^{23},Nle^{21,38}]h/rCRF$_{12-41}$	88	3.6 at 33.6	85	-70	3435.93	3436.2	0.11 (0.035-0.34)	5
38	cyclo(20-23)[DPhe^{12},Asp^{20},Orn^{23},Nle^{21,38}]h/rCRF$_{12-41}$	98#	3.8 at 36.6	98	-68	3463.97	3464.0	0.04 (0.02-0.07)	4

[a] Percent purity determined by HPLC using buffer system. A: TEAP (pH 2.5). B: 60% CH_3CN/A with a gradient slope of 1% B/min, at flow rate of 1.5 mL/min on a Vydac C_{18} column (0.46 × 25 cm, 5-μm particle size, 300-Å pore size or (#) at flow rate of 0.2 mL/min on a Vydac C_{18} column (0.21 × 15 mm. 5-μm particle size, 300-Å pore size). Detection at 210 nm. [b] Isocratic retention times in minutes using buffer system. A: 0.1% TFA/H_2O. B: 0.1% TFA in CH_3CN/H_2O (60:40). Results are reported in terms of retention time at a shown concentration of CH_3CN at 2 mL/min using a Vydac C_{18} column (0.46 × 25 cm, 5-μm particle size, 300-Å pore size). Detection at 210 nm. [c] Field strength of 15 kV at 30 °C, mobile phase: 100 mM sodium phosphate pH 2.50, on a fused silica capillary (363-μm o.d. × 75-μm i.d. × 60-cm length). Detection at 214 nm. [d] Measured in 1% or in 50% (‡) acetic acid. [e] The observed m/z of the monoisotope compared with the calculated $[M + H]^+$ monoisotopic mass. The average m/z compared with the calculated $[M + H]^+$ average mass is indicated by an asterisk (*). [f] Potencies are relative to that of [DPhe^{12},Nle^{21,38}]rCRF$_{12-41}$, with 95% confidence limits in parentheses. [g] Intrinsic activity expressed as a percent of that of oCRF.

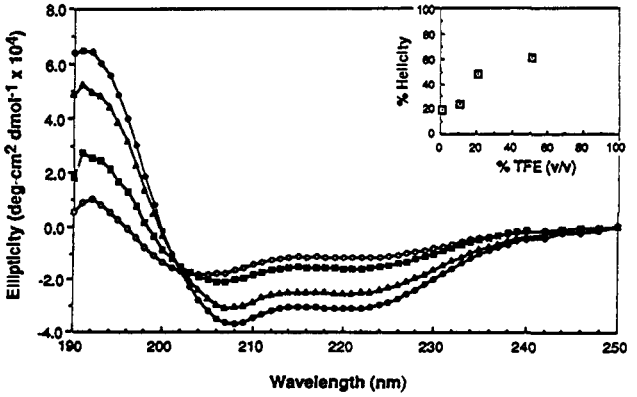

Figure 1. CD spectrum of the standard, [DPhe^{12},Nle^{21,38}]rCRF$_{12-41}$ as a function of the concentration of TFE: 0% TFE, open circles; 10% TFE, closed boxes; 20% TFE, open triangles; 50% TFE, closed circles. Insert: The theoretical helical content at varying concentrations of TFE was calculated by the method of Yang et al.[46]

of TFE, plotted in the inset to Figure 1, attains a value of 62% at a TFE concentration of 50% (v/v). This value is lower than the expected one (76%) based on NMR studies of r/hCRF carried out under very similar conditions by Romier et al. and where they found that the extended N-terminal (residues 1-5) connected to a well-defined α-helix between residues 6 and 36 with the five C-terminal residues assuming no structure or the 78% helicity found in 100% TFE for the whole human/rat CRF using CD.[34] Thus, we judged that zero and 50% TFE would be convenient standard concentrations for investigating the effect of side chain bridge introduction on peptide secondary structure. Consequently, the CD spectra of all of the cyclic compounds reported here, with the exception of **23**, were measured in aqueous and 50% TFE solution. As shown in Table 2, significant β sheet and random coil type structures characterize all of the compounds under aqueous conditions with only compounds **6**, **9**, and **16** having α-helical structure in excess of 20%. Alternatively, in 50% TFE, significant α-helical structure is induced in all compounds with concomitant reduction in β sheet and turn structures. No obvious correlation can be found between biological activity and secondary structural features observed in CD.

Molecular Modeling. As a heuristic aid in the design

Table 2. Calculated Secondary Structural Components in Aqueous and 50% TFE solution[a]

	aqueous solution				50% TFE solution			
compd	α	β	turn	random	α	β	turn	random
1	0.07	0.44	0.03	0.46	0.62	0.00	0.00	0.38
2	0.09	0.46	0.00	0.44	0.58	0.00	0.00	0.42
3	0.12	0.26	0.06	0.57	0.58	0.00	0.00	0.42
4	0.12	0.22	0.11	0.55	0.70	0.00	0.00	0.30
5	0.10	0.24	0.08	0.58	0.62	0.00	0.00	0.38
6	0.32	0.26	0.00	0.42	0.69	0.00	0.00	0.31
7	0.00	0.50	0.00	0.50	0.56	0.00	0.00	0.44
8	0.19	0.26	0.12	0.43	0.65	0.00	0.00	0.35
9	0.21	0.28	0.08	0.43	0.65	0.00	0.00	0.35
10	0.04	0.26	0.09	0.61	0.57	0.00	0.00	0.43
11	0.03	0.32	0.10	0.55	0.53	0.00	0.00	0.47
12	0.00	0.48	0.00	0.52	0.51	0.01	0.00	0.48
13	0.06	0.48	0.00	0.45	0.67	0.00	0.00	0.33
14	0.06	0.47	0.00	0.47	0.67	0.02	0.00	0.31
15	0.03	0.35	0.05	0.57	0.69	0.00	0.00	0.31
16	0.26	0.00	0.13	0.61	0.89	0.00	0.00	0.11
17	0.06	0.27	0.10	0.57	0.65	0.00	0.00	0.35
18	0.00	0.35	0.09	0.56	0.53	0.00	0.00	0.47
19	0.00	0.34	0.08	0.58	0.62	0.00	0.00	0.38
20	0.02	0.37	0.08	0.53	0.40	0.12	0.00	0.48
21	0.00	0.45	0.05	0.50	0.41	0.04	0.00	0.55
22	0.00	0.38	0.12	0.50	0.40	0.09	0.03	0.48
23	ND				ND			
24	0.00	0.44	0.06	0.50	0.34	0.28	0.00	0.38
25	0.00	0.60	0.00	0.39	0.42	0.17	0.00	0.41
26	0.00	0.46	0.08	0.46	0.47	0.16	0.00	0.37
27	0.00	0.44	0.06	0.50	0.38	0.11	0.00	0.51
28	0.00	0.24	0.18	0.58	0.50	0.00	0.00	0.50
29	0.00	0.39	0.08	0.53	0.62	0.00	0.00	0.38
30	0.06	0.19	0.12	0.62	0.50	0.00	0.00	0.50
31	0.08	0.19	0.14	0.59	0.51	0.00	0.00	0.49
32	0.04	0.35	0.06	0.55	0.50	0.00	0.00	0.50
33	0.19	0.06	0.019	0.56	0.59	0.00	0.00	0.41
34	0.06	0.53	0.00	0.41	0.52	0.09	0.00	0.39
35	0.06	0.57	0.01	0.37	0.47	0.03	0.00	0.50
36	0.07	0.23	0.12	0.58	0.61	0.00	0.00	0.39
37	0.05	0.27	0.12	0.56	0.46	0.06	0.00	0.48
38	0.00	0.58	0.01	0.41	0.33	0.24	0.00	0.43

[a] Spectra were deconvoluted with the program PROSEC (Aviv Associates) using the reference spectra of Yang et al.[46]

and optimization of side chain bridging functions, the structural consequences of the introduction of $i-(i+3)$, $i-(i+4)$, and $i-(i+5)$ disulfides or lactams of varying bridge length were investigated. A computer model of an idealized α helical conformation [(ψ,ϕ) = (-65,-40)] of tetradecaalanine was constructed. This structure was mutated in turn by the introduction of Cys, Asp, or Glu at position 5 and Cys, Dpr, Dbu, Orn, Lys at positions 8–10 to yield the corresponding $i-(i+3)$, $i-(i+4)$, or $i-(i+5)$ bridges. The mutated structures were allowed to relax by flexible geometry energy minimization to a maximum derivative of 0.1 kcal/(mol/A) and the resulting Cα–Cα distances between the bridgeheads were calculated. In order to quantitate the degree of distortion to the α-helical structure caused by the bridge, the rms deviations with respect to the ideal α-helix over the backbone atoms of the residues involved in the cyclic bridged substructures were calculated. These data are reported in Table 3.

Biological Activity. CRF analogues were tested for antagonist activity in an *in vitro* assay measuring alteration of CRF-induced release of ACTH by rat anterior pituitary cells in culture.[47] The relative potency of each cyclic antagonist is reported in Table 1. Each value represents the mean ± the standard error of the mean (SEM) of triplicate wells. Relative potencies with 95% confidence limits in parentheses are shown with [DPhe^{12},Nle^{21,38}]h/rCRF$_{12-41}$ = 1.

Table 3. Cα–Cα Distances between $i-(i+3)$, $i-(i+4)$, or $i-(i+5)$ Bridgeheads Derived from a Computer Model of an Idealized α-Helical Conformation [(ψ,ϕ) = (-65,-40)] of tetradecaalanine[a]

	$i-(i+3)$		$i-(i+4)$		$i-(i+5)$	
bridge type	Cα–Cα	rms	Cα–Cα	rms	Cα–Cα	rms
Cys–Cys	4.22	0.67	4.58	1.16	4.87	1.94
Asp–Dpr	4.46	0.46	4.63	1.40	4.58	2.33
Asp–Dbu	5.19	1.09	5.48	1.47	4.96	2.26
Asp–Orn	4.83	0.45	5.55	1.08	5.14	1.95
Asp–Lys	4.68	0.33	5.51	0.58	6.33	1.44
Glu–Dpr	4.76	0.28	5.13	0.70	5.26	1.93
Glu–Dbu	4.64	0.29	5.36	0.80	5.66	1.64
Glu–Orn	4.84	0.23	5.79	0.55	6.06	1.46
Gly–Lys	4.72	0.17	5.87	0.36	6.75	1.21
DCys–Cys	5.38	0.13	5.48	0.99	5.05	1.86
DAsp–Dpr	5.12	0.25	5.12	1.26	5.20	2.21
DAsp–Dbu	5.38	0.31	5.90	1.15	5.71	2.05
DAsp–Orn	6.06	0.75	5.86	0.80	5.89	1.75
DAsp–Lys	5.54	0.45	6.03	0.58	6.57	1.50
DGlu–Dpr	5.38	0.13	5.55	0.56	5.39	1.93
DGlu–Dbu	5.82	0.36	5.83	0.98	5.75	1.68
DGlu–Orn	5.49	0.26	5.86	0.62	6.16	1.53
DGlu–Lys	5.43	0.17	6.27	0.60	6.75	1.41
Cys–DCys	3.71	0.36	4.08	0.71	4.15	1.90
Asp–DDpr	4.81	0.65	4.39	0.68	4.73	1.83
Asp–DDbu	3.94	0.33	4.49	0.58	4.29	1.90
Asp–DOrn	4.02	0.33	5.10	0.37	4.46	1.86
Asp–DLys	4.04	0.31	4.73	0.55	6.04	1.27
Glu–DDpr	4.23	0.34	4.22	0.70	4.84	1.64
Glu–DDbu	3.90	0.31	4.07	0.84	5.62	1.36
Glu–DOrn	3.98	0.31	5.25	0.36	6.03	1.29
Glu–DLys	4.16	0.26	6.03	0.09	6.63	1.01
DCys–DCys	4.23	0.29	4.83	0.57	4.82	1.65
DAsp–DDpr	4.49	0.35	4.67	0.72	4.82	1.73
DAsp–DDbu	4.58	0.30	5.25	0.41	5.19	1.62
DAsp–DOrn	4.69	0.23	5.31	0.48	5.42	1.59
DAsp–DLys	4.90	0.27	5.36	0.41	6.17	1.31
DGlu–DDpr	5.38	0.46	5.17	0.46	5.08	1.61
DGlu–DDbu	4.61	0.24	5.02	0.62	5.51	1.48
DGlu–DOrn	4.69	0.19	5.42	0.41	6.02	1.39
DGlu–DLys	4.93	0.14	5.47	0.49	6.45	1.19

[a] This structure was mutated in turn by the introduction of Cys, Asp, or Glu at position 5 and Cys, Dpr, Dbu, Orn, and Lys at positions 8–10. Idealized Cα–Cα distances between $i-(i+3)$, $i-(i+4)$, or $i-(i+5)$ in an α-helix are 5.23, 6.18, and 8.75 Å, respectively.

Discussion

While short bioactive compounds are not observed to assume helical structures, helicity and amphiphilicity often seem to characterize long peptides. Because physicochemical evidence suggests that CRF assumes an α-helical structure in solution, we have searched for structural constraints that would unequivocally lock the structure into such conformation. Side chain–side chain bridging offers such opportunity. Whereas Felix et al. took advantage of putative salt bridges as the rationale for the location of bridgeheads in GRF,[40] we introduced (in CRF) bridgeheads at such locations (positions 20 and 23) as well as at positions where (at least for one of the bridgeheads) a D-residue increased potency (positions 12 and 20). These substitutions were guided by model studies based on Cα–Cα distances shown in Table 3 and on a model of [DPhe^{12},Nle^{21,38}]h/rCRF$_{12-41}$ originally constructed in an ideal α-helix and subsequently relaxed. Of interest was the distribution of hydrophobic and hydrophilic residues in this idealized structure. As shown in Figure 2A, the N-terminal region from DPhe^{12} to Arg^{23} is very polarized, with DPhe^{12}, Leu^{14,15,19}, Val^{18}, Nle^{21}, and Ala^{22} describing the hydrophobic face, opposed by His^{13}, Arg^{16}, Glu^{17,20}, and Arg^{23} forming the hydrophilic face. This is a

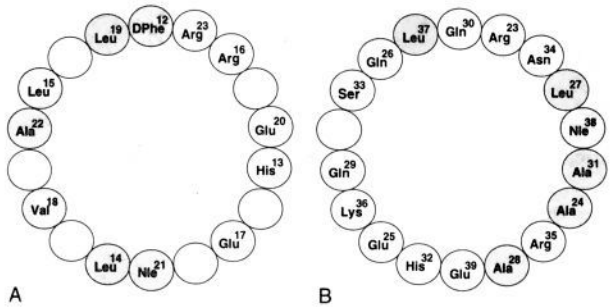

Figure 2. Helical wheel diagrams of regions of [DPhe^{12},-Nle^{21,38}]h/rCRF$_{12-41}$: (A) residues 12–23; (B) residues 23–39. Hydrophilic residues are not shaded. Hydrophobic residues are shaded dark gray. Positions on the helical wheel which are not filled are shaded light gray. Both diagrams are in the same registration.

configuration (amphipathic helix) that was also observed using NMR.[38] The hydropathy of these faces then "switches" sides (Figure 2B) with a hydrophobic stretch evident involving Ala^{24,28,31} and Leu^{27}, which is disrupted by the Asn^{34}–Arg^{35} pair but continues through to Nle^{38}. Dominating the other face of the C-terminal half of the molecule is the hydrophilic region composed of Glu^{25,39}, Gln^{26,29,30}, His^{32}, Ser^{33}, and Lys^{36}. The molecule is maximally hydrogen bonded, with every carbonyl oxygen from DPhe^{12} through Leu^{38} (two residues beyond the α-helix shown to be present by NMR in hCRF) hydrogen bonded to the corresponding $i-(i+4)$ amide proton.

Considering the above, we determined that a compatible bridging unit to stabilize an α-helix would be a cystine residue or a pair of complementary residues such as Glu or Asp and Lys linked through their side chains in an $i-(i+3)$, $i-(i+4)$, or $i-(i+5)$ configuration. Our initial attempts at achieving $i-(i+3)$ cyclization via disulfide bridges (**1–4**) uniformly resulted in compounds with low relative potencies. Upon examination of Table 3 and our recognition that an ideal helix would have a Cα–Cα distance of 5.23 Å, only **4** with DCys^{12}-Cys^{15} with a Cα–Cα distance of 5.38 Å should have shown significant activity. All other analogues in that series (**1–3**) have predicted Cα–Cα distances shorter by at least 1.0 Å. In order to determine whether a specific Cys side-chain effect was responsible for the low potency of **4** with DCys^{12},Cys^{15}, we synthesized **5** with DGlu^{12}-Lys^{15} and found it to be equally inactive. Because the $i-(i+3)$ failed to yield at first view an active analogue, we synthesized the corresponding $i-(i+4)$ cyclo(12–16) analogue **6** (DGlu^{12}-Lys^{16}) which according to Table 3 would easily assume an α-helical structure. Interestingly, **6** is 25 times more potent than **5**. The fact that no increase in potency was observed as a result of substituting this bridging modality (compare **5** to **4**), while an increase in potency was observed as the result of increasing the size of the bridge [$i-(i+3)$ *vis a vis* $i-(i+4)$] (compare **5** to **6**), suggests significant sensitivity of the receptor to such structural perturbation and that further optimization could be obtained unless side chains at these positions are necessary for receptor binding as demonstrated in our earlier study of the alanine scan of oCRF.[48]

To implement a general principle that would allow identification of effective bridgeheads for stabilization of α-helices (i.e., use the knowledge that a D-residue is allowed at a given position), we have concentrated our efforts around position 20 since [DGlu^{20}]oCRF was found to be 1.5 times more potent than oCRF.[45] Using position 20 as a pivot point, we investigated bridges between [$(i-5,-4,-3)-i$)] (**7–21**) and between [$i-(i+3,+4,+5)$] (**22–38**).

Whereas in an ideal α-helix the $i-(i+5)$ Cα–Cα distance is about 8.75 Å (see Table 3), we hypothesized that **7** with a cyclo(15–20) Lys^{15}-Glu^{20} would have the highest probability of exhibiting activity in the cyclo 15–20 series. The fact that this analogue was inactive at the doses tested argued strongly against further exploration of this series. While **7** was inactive at the doses tested, we investigated the next possible bridging opportunity by introduction of a 16–20 bridge in the four possible Lys^{16}-Glu^{20} enantiomeric pairs (**8**, **13–15**). Interestingly, the two most potent analogues (40%), **8** and **15**, employ L-Lys^{16} and differ in chirality at position 20, which is consistent with data in Table 3 showing that both D and L configurations were allowed (Cα–Cα distances of 5.87 and 6.03 Å versus 6.18 Å with insignificant RMS deviations, 0.36 and 0.09 Å, respectively). We interpret this as evidence for significant side chain bridge flexibility of this bridging modality. Introduction of D-Lys^{16} resulted in analogues **13** and **14** with 8 and 21% potency and theoretical Cα–Cα distances of 6.27 Å (rms = 0.60 Å) and 5.47 Å (rms = 0.49 Å), respectively.

At this stage of development of this line of SAR, we thought it necessary to further test our hypothesis based on distances shown in Table 3. The most obvious approach would be to reduce the size of the bridge as defined in **8**. We found that reduction of ring size in **8** by one methylene results in **9** with ca. half its potency. Maintenance of the ring size but displacement of the bridging amide bond (**10**) did not affect potency, suggesting that contrary to what was observed in another system (GnRH),[37] positioning of the amide bond does not influence receptor/ligand interaction. Further contraction of this ring (**11–12**) significantly decreased potency (2.1 and 0.1%, respectively). In summary, it is apparent that reducing the size of the ring by two carbon units, which would result in a relatively small theoretical difference in Cα–Cα distances (5.87 to 5.36 Å), resulted in significant loss of potency (40% to 2%). Because of the observation that **8** and **15** were equipotent, it raised the question as to whether a smaller ring (such as that found in **16** and **17**) than that found in the above two analogues with a D residue at the $i+4$ position would be more favorable. Biological results of **16** and **17** indicate again that reduction of ring size gradually results in less potent analogues (6% and 0.6%, respectively).

Further constriction of the ring size [$(i-3)-i$] with the introduction of the L–L and L–D configurations found earlier to be favorable (**8** and **15**) resulted in lactams **18** and **19** with very low (2%) or negligible (<0.1%) relative potencies. Because of the observation that the introduction of a Dbu-Asp bridge (5.19 Å) would theoretically result in a larger Cα–Cα distance than a Glu-Lys bond (4.72 Å), we also synthesized **20** which showed low potency (0.5%). Similarly, introduction of a Cys bridge (**21**) in this same [$(i-3)-i$] position (resulting in a further constriction of the ring size) also led to an inactive analogue. We had erroneously reported **21** to have 50% relative potency in an earlier communication[37] in which the standard (used for this particular analogue only) was α-helical-CRF$_{9-41}$. This analogue, recently retested against [DPhe^{12},Nle^{21,38}]h/rCRF$_{12-41}$, was found to be less than 1% as potent as the standard. This further demonstrates that introducing in this region of the molecule a shorter ring than the one

found in the active analogues 8 and 15, and conformational constraints such as those resulting from the introduction of a Cys–Cys bridge, consistently result in loss of potency.

At this point, it may be important to realize that first examination of Table 3 may suggest discrepancies in the relative distances reported. We reiterate that the tetradecaalanine models were built in vacuum and that the computational procedure was limited to flexible geometry minimization.[49] The practical implications are that the trends in the predicted lengths of bridges may be correct although allowing specific exceptions. For example, the Cα–Cα distance of Cys–Cys bridges tend to be the shortest while the Cα–Cα distance of Glu–Lys bridges the longest. This is without saying that in our series of CRF analogs, side chain–side chain interactions of the different amino acid in the sequence must play a significant role in directing conformation and in interacting with the CRF receptor.

Having examined $(i - 5, -4, -3) - i$ bridges with Glu^{20} as the pivot point i, our next goal was to investigate the effect of the introduction of a bridge further down the sequence with a series of $i - (i + 5, +4, +3)$ bridged analogues with Glu^{20} again as the pivot point.

The largest ring structure (equivalent to that found in 7) is found in **22** $[i - (i + 5)]$ which retains 5% relative potency. Whether such retention of activity is due to differences in chirality of the bridges or to other specific receptor interactions is presently being investigated. The Glu–Lys bridge seems to be tolerated despite the fact that Cα–Cα distances between residues 20 and 25 would be ca. 9 Å in an ideal α-helix (Table 3). This suggests that this bridge does not drastically perturb the α-helical structure in the $[i-(i+5)]$ context (which is confirmed by molecular modeling) or that the receptor is permissive of such perturbations.

Systematic contraction of the ring along the backbone (**23** and **24**) resulted in an incremental improvement in biopotency (20 and 50%, respectively). Systematic chiral optimization (**24–27**) of the bridge heads at positions 20 and 23 resulted in the most potent cyclic CRF analogue reported so far (**25**, 290%). This may be best explained by the presence in rCRF of an arginine in position 23 which is likely to participate in a salt bridge with Glu^{20} in the active conformer. Indeed, stabilizing this interaction by a covalent amide bridge resulted in a highly potent antagonist, suggesting that the bridging unit increased stability of the active conformer. Similar observations had been made by Felix et al. in a series of growth hormone-releasing factor analogues.[50] Any disruption of the conformation in which the effect of changes in chirality has been systematically investigated (as in **24**, **26** and **27**) yielded less potent analogues. Interestingly, introduction of $DGlu^{20}$ resulted in a 6-fold decrease in potency (compare **25** and **24**), whereas a similar substitution in **15** caused no decrease in potency with a 17/20 bridge (compare **8** and **15**). Introduction of DLys at position 23 (**27**) has a dramatic effect (150-fold) on biopotency as compared to the lack of effect of its introduction in the $DGlu^{20}$-containing analogues **24** and **26** (both analogues being approximately half as potent as the standard).

Further improvement in biopotency has been achieved in the development of GnRH analogues by inversion of the direction of the bridging amide.[37] This observation served as the basis for the synthesis of **28** and **29** which incorporated a Lys and DLys at position 20, respectively. While both analogues are equipotent (12%) (a result that could have been in part anticipated by the fact that both a D- and LGlu are tolerated at position 20), a significant loss of potency (24-fold comparing **25** to **28** and 4-fold comparing **24** to **29**) resulted from this modification. We have attributed such changes in potencies resulting from amide bond reversal to changes in enzymatic stability, or simply to an as yet undefined receptor linked property. Additionally, in the case of an α-helix, one could speculate that changes in the direction of an amide bond could result in the introduction of a stabilizing/destabilizing dipole.[51]

Another variable that may result in dramatic changes in potency is ring size and positioning of the amide bridge on that ring. In **30–38**, we have investigated the influence of ring contraction by reducing the length of the bridging side chains in ways that also allow displacement of the amide bridge toward or away from the N-terminal bridge head. Reduction of the ring in **24** by one or three methylenes (compare **24** to **30** and **31**) actually results in a nonstatistically significant 2-fold decrease in potency while the predicted Cα–Cα distances for the three analogues are essentially the same (5.43, 5.49, and 5.38 Å). While substitution of Lys^{23} by Orn^{23} (**32**) resulted in a statistically nonsignificant reduction of potency from 3-fold for **25** to 2-fold that of the standard, reduction of the ring size by introduction of Asp^{20} and Lys^{23} (**33**) led to a completely inactive analogue (theoretical Cα–Cα distance = 4.68 Å). Interestingly, **34** with a $D\text{-}Asp^{20}$ regained 2.2% potency relative to the standard (theoretical Cα–Cα distance = 5.54 Å). The ideal theoretical Cα–Cα distance for an $i-(i+3)$ bridge being 5.23 Å, a value closer to that calculated for **34**, suggested that this approach may have some predictive value as also shown above. Reducing the ring size further by the introduction of Orn^{23}, Dbu^{23}, and Dpr^{23} in **35–37** resulted in two of the most potent analogues in this series (**35** and **36**) and a relative 4-fold loss of potency for **37** although this difference is not statistically significant. In this case, the theoretical $i-(i+3)$ Cα–Cα distance for the DAsp–Orn bridge found in **35** being 6.06 Å, 5.38 Å for the DAsp–Dbu bridge found in **36**, and 5.12 Å for the DAsp–Dpr bridge found in **37**, which compare with 5.23 Å found in the polyalanine model, the optimized structures would not have been predicted by the calculation. This reiterates the need for exploratory chemical optimization.

The fact that Asp^{20}-Orn^{23} (**38**) retained some potency (4%) suggested that the actual placement of the lactam function relative to the backbone, or other important conformational or functional side chains, was crucial. For example, comparison between **35** and **38** indicated that chiral inversion of Asp^{20} resulted in a 10-fold reduction in potency. On the other hand, deletion of a methylene group in the bridges of **30** and **35** with the D-chirality in position 20 had no statistically significant effect on biopotency (20% and 40%, respectively).

Conclusion

In this paper, we have addressed several hypotheses relating to the mechanism of CRF binding. First, bridge-heads can be located at positions where a D-residue is allowed provided that bridge length, chirality, and direction are optimized. Second, we suggest that this effect is mediated through stabilization of an α-helical structure, a hypothesis which is compatible with the observation that all these structures can assume an α-helical conformation in the presence of TFE. Third, by assuming an

α-helical bioactive structure for CRF, a simple predictive tool based on Cα–Cα distances in an ideal polyalanine α-helical model was developed. We have used this model and found it to have some predictive value. In two cases, we obtained cyclic analogues with potencies slightly greater than that of a related linear compound, which suggests that restricted conformational freedom is compatible with strong antagonist binding. Finally, most of the active analogues presented here still showed some intrinsic activity for which we have no explanation. It was hoped that, as had been observed in the case of GnRH (Rivier et al., unpublished results), introduction of structural constraints would reduce intrinsic activity.

Experimental Section

Materials. All reagents and solvents for solid-phase peptide synthesis were analytical grade and were used from freshly opened containers without further purification. Reagent-grade trifluoroacetic acid (TFA) purchased from Halocarbon Products Corp. (Hackensack, NJ) and triethylamine (TEA) purchased from Aldrich Chemical Co., Inc. (Milwaukee, WI) were distilled for further use in the preparation of chromatographic buffers. Dimethylformamide (DMF) purchased from Mallinckrodt Inc. (Paris, KY) was dried and stored over molecular sieves (Type 3A, $^1/_{16}$-in. pellets, Eastman Kodak Co., Rochester, NY), and before use a nitrogen steam was applied to remove volatile amines. Boc-amino acids were purchased from Bachem (Torrance, CA). Side chain protecting groups were: Arg(Tos), Asp(β-OcHex or β-OFm), Cys(S-*p*-Mob), Glu(γ-OcHex or γ-OFm), His(Tos)·DCHA, Lys(ε-2ClZ or ε-Fmoc), Orn(Fmoc), Ser(Bzl,) and Thr(Bzl). The N^{α}-Boc-L-Dpr(Fmoc) was synthesized in our laboratory according to the method of Almquist et al.[52] The reagents 1,3-diisopropylcarbodiimide (DIC), 1-hydroxybenzotriazole (HOBt), anisole, acetic anhydride, and diisopropylethylamine (DIEA) were purchased from Aldrich; acetonitrile (CH_3CN) (reagent grade and ChromAR HPLC grade) and 2-propanol (i-PrOH) were purchased from Mallinckrodt; methanol (MeOH) and dichloromethane (DCM) were purchased from Fisher Scientific Co. (Fair Lawn, NJ); ethanedithiol (EDT) was purchased from Fluka Chemie AG (Switzerland); (benzotriazol-1-yloxy)tris(dimethylamino)phosphonium hexafluorophosphate (BOP) was purchased from Richelieu Biotechnologies, Inc. (Quebec, Canada).

General Method for Peptide Synthesis. The resin-bound peptides incorporating the Boc-protected amino functions were synthesized manually by solid-phase. Methylbenzhydrylamine-resin (MBHA-resin) was prepared in our laboratory[42] from polystyrene cross-linked with 1% divinylbenzene (Biobeads SX-1, 200–400 mesh, Bio-Rad Laboratories, Richmond, CA). Resins with substitutions varying from 0.43 to 0.46 mequiv/g were used. The N^{α}-terminal protection was deblocked with trifluoroacetic acid–dichloromethane (TFA–DCM) (3:2) in the presence of 1% ethanedithiol (EDT) for 20 min, followed by washes with 2-propanol (i-PrOH) containing 1% ethanedithiol (EDT) (2×), 10% triethylamine (TEA) in dichloromethane (DCM) (2×), methanol (MeOH) (2×), 10% triethylamine (TEA) in dichloromethane (DCM) (2×), methanol (MeOH) (2×), and dichloromethane (DCM) (3×). Coupling was mediated using a 2.5-fold excess of Boc-amino acid/1,3-diisopropylcarbodiimide (DIC) (1:1) (based on the degree of substitution of the resin) in dichloromethane (DCM) or dichloromethane–dimethylformamide (DCM–DMF) (1:1, v/v), depending on the solubility of the Boc-amino acid derivative. Asparagine and glutamine couplings were done using a 1.5-fold excess of 1-hydroxybenzotriazole (HOBt) and His(Tos)·DCHA with a 1.5-fold excess of BOP[43] in presence of excess of diisopropylethylamine. All couplings were monitored by using the Kaiser ninhydrin test.[53] Coupling time was for 1–4 h, with recouplings done where needed using BOP in the presence of excess diisopropylethylamine (DIEA) (pH maintained between 8 and 9 during the reaction) in dimethylformamide (DMF) or dichloromethane–dimethylformamide (DCM–DMF) (1:1, v/v) generally for 1 h. When needed, acetylation was performed with acetic anhydride 50% in dichloromethane (DCM) for 10 min.

The dry protected peptide-resin was cleaved in liquid HF in the presence of 3–10% anisole at 0 °C for 90 min. Excess HF and scavenger were eliminated under high vacuum (discoloration of the resin from bright red to yellow). The crude peptides were precipitated with anhydrous diethyl ether, separated from ether-soluble nonpeptide material by filtration, extracted from the resin with 0.1% TFA in CH_3CN/H_2O (60:40) and lyophilized.

Peptide Cyclization. Solid-phase side chain to side chain cyclization (lactamization) of the peptide on the resin was performed by the method of Felix et al.[40] After washes with dichloromethane (DCM) (2×), dimethylformamide (DMF) (2×), the OFm/Fmoc groups were removed by 20% piperidine in dimethylformamide (DMF) (1 × 1 and 2 × 10 min), followed by washing with dimethylformamide (DMF) (2×), methanol (MeOH) (2×), and dichloromethane (DCM) (2×). The peptide-resin was cyclized by reaction with 3-fold excess of (benzotriazol-1-yloxy)-tris(dimethylamino)phosphonium hexafluorophosphate (BOP) in the presence of excess diisopropylethylamine (DIEA) in *N*-methylpyrrolidone (NMP). After washing the cyclization was repeated every 4 h (12 h overnight). The reaction was followed by Kaiser ninhydrin[53] test and in general was completed after 24–30 h.

Cyclization of free sulfhydryl-containing analogues was performed following HF cleavage. After removal of HF under reduced pressure, the resin was washed with diethyl ether in portions. The peptide was quickly extracted from the resin (H_2O and 5.0% AcOH), the solutions diluted with water, the pH adjusted to 6.8–7.0 with NH_4OH, and the mixture allowed to stir slowly and air oxidize at 4 °C. The completion of cyclization was followed by the Ellman test and by RPHPLC. After 2–3 days the cyclization was completed, the solution was acidified to pH 5.0 and applied to a Bio-Rex-70 column, and the peptide was eluted with 50% AcOH. The peptide-containing fractions were pooled and lyophilized.

Peptide Purification. The crude lyophilized peptides were purified by preparative reverse-phase HPLC (RPHPLC)[44,54] on a system composed of a Waters Associates (Milford, MA) Prep LC 3000 System, a Waters Associate 600E System Controller, a Shimadzu SPD-6A UV spectrophotometric variable-wavelength detector (detection was at 230 nm), Waters 1000 PrepPak Module, and a Fisher (Lexington, MA) Recordall Series 5000 strip chart recorder (chart speed 0.25 cm/min). Peptide purification was accomplished in two (TEAP 2.25 and 0.1% TFA) or three steps (TEAP 2.25, TEAP 5.0–6.0, and 0.1% TFA). Crude peptides were dissolved in acetonitrile/triethylammonium phosphate (TEAP) buffer (1:4 v/v), loaded on a preparative reversed-phase HPLC cartridge (5 × 30 cm) packed in our laboratory using Waters polyethylene sleeves and frits and Vydac C_{18} silica gel (The Separations Group, Hesperia, CA; 300-Å pore size, 15–20-μm particle size). The peptide was eluted using an appropriate gradient (slope 0.33% B/min) inferred from the analytical results. Buffers A (triethylammonium phosphate (TEAP), pH 2.25) and B (60% CH_3CN in A) were pumped at a flow rate of 95 mL/min such that elution time of the desired peptide was between 30 and 45 min. Individual fractions were collected and analyzed by RPHPLC under isocratic conditions [Vydac C_{18} silica gel column, 0.46 × 25 cm, 5-μm particle size, 300-Å pore size, solvents A, 0.1% TFA/H_2O, and B, 0.1% TFA in CH_3CN/H_2O (60:40), at a flow rate of 2.0 mL/min, detection at 210 nm], such that the retention time was between 3 and 5 min. Selected fractions were collected and diluted (1:1) with water and loaded on a preparative cartridge as above and eluted using a linear gradient (slope 0.33% B/min) containing a mixture of solvents A (TEAP, pH 5.0 to 6.5) and B (60% CH_3CN in A) at a flow rate of 95 mL/min. Individual fractions were analyzed as above under isocratic conditions and selected fractions diluted (1:1) with water. These fractions were converted to the TFA salt by loading on a preparative cartridge as above and eluted using a linear gradient (slope 0.33% B/min) containing a mixture of solvents A (0.1% TFA/H_2O) and B [0.1% TFA in CH_3CN/H_2O (60:40)] at a flow rate of 95 mL/min. Selected fractions, containing the purified peptide, were pooled and lyophilized.

Synthesis and Purification of Cyclo(20–23)[dPhe^{12},Glu^{20},-Lys^{23}, Nle^{21,38}]h/rCRF$_{12-41}$ (25). According to the protocol described earlier in this section, 2 g (0.43 mequiv/g) of MBHA resin was deprotected and neutralized. Completion of couplings

(1–4 h) was monitored by ninhydrin test. His[32], Gln[26], Ala[22], Nle[21], Val[18], Glu[17], Arg[16], and Leu[14] required a recoupling step. Arg[35], Asn[34], Ser[33], Glu[25], Ala[24], Leu[19], and Leu[15] required a double recoupling. Arg[35], Asn[34], Gln[26], and Ala[22] required acetylation after coupling. After incorporation of the last amino acid, the OFm/Fmoc groups of Glu[20] and Lys[23], respectively, were removed. The formation of the bridge was accomplished in 24 h (negative ninhydrin test) after four treatments (3 for 4 h and 1 for 12 h) with fresh coupling reagents (BOP/DIEA) at room temperature. After removal of the N^{α}-Boc protecting group a fully protected peptide-resin was dried. A total of 4.8 g was obtained, 2 g was cleaved by anhydrous HF (20 mL) in the presence of anisole (0.6 mL) at 0 °C for 90 min. The crude peptide was precipitated and washed with anhydrous diethyl ether (450 mL in 3 portions), filtered, extracted from the resin with 380 mL (4 portions) of 0.1% TFA in CH_3CN/H_2O (60:40) and lyophilized to give 1.02 g of crude product. Purification was performed in two stages as described earlier. First the peptide was dissolved in 400 mL of buffer A (TEAP pH 2.25) and eluted with buffer B (60% CH_3CN in A), with a gradient from 30 to 60% B in 90 min (retention time was ca. 36 min). A total of 20 fractions containing 50–100 mL were screened under isocratic conditions (61% B, retention time was ca. 4.2 min), and three acceptable fractions (numbers 30–32) containing the compound were identified and pooled. In the second step, the pooled fractions (ca. 160 mL) were diluted with 160 mL of H_2O, were loaded and eluted by using as buffer A (0.1% TFA/H_2O) and B (0.1% TFA in CH_3CN/H_2O (60:40)), with a gradient from 40 to 70% B in 90 min (retention time was ca. 60 min). A total of 19 fractions containing 30–50 mL each were screened, five fractions (160 mL, numbers 17–21) were pooled and lyophilized to yield **25** (yield = 70.9 mg: 3.6% of expected amount from the original substitution of the MBHA resin).

Synthesis of **5–20** and **22–38** proceeded in a similar manner.

Cyclization and Purification of Cyclo(20–23)[dPhe[12],-Cys[20],Cys[23],Nle[21,38]]h/rCRF[12–41] (21). According to the synthesis protocol described earlier in this section, 1.9 g of the fully protected peptide-resin was cleaved by HF. After precipitation and washing with diethyl ether (ca. 480 mL in three portions), the peptide was extracted with water (200 mL) and 5% AcOH (100 mL). The resulting solution was poured into 4.0 L of degassed water and the pH adjusted to 6.8–7.0 with NH_4OH. As the mixture became cloudy, CH_3CN (300 mL) was added to avoid precipitation. The mixture was then stirred at 4 °C, and after 48 h the cyclization was completed (Ellman test). The pH was adjusted to 5.0 with AcOH, and the resulting solution was loaded on a Bio-Rex-70 column (120 mL). The column was washed with 0.5% AcOH (200 mL) and the peptide eluted with 50% AcOH. Fractions were collected, and those containing ninhydrin positive material were diluted and lyophilized (800 mg). Purification was performed in three steps. First the peptide was dissolved in buffer A (TEAP pH 2.25, 300 mL) and eluted with buffer B (60% CH_3CN in A) and a gradient from 30 to 60% B in 60 min (retention time was ca. 32 min). A total of 10 fractions was screened under isocratic conditions (53% B, retention time 3.7 min), and three acceptable fractions containing the compound were pooled. In the second step the pooled fractions (ca 150 mL) were diluted with H_2O (150 mL) and eluted using buffer A (TEAP 6.0) and B (60% CH_3CN in A), with a gradient from 30 to 55% B in 60 min (retention time was ca. 25 min). A total of 24 fractions were screened under isocratic conditions (53% B). The pooled fractions (17–23) were diluted with H_2O and eluted using buffer A (0.1% TFA/H_2O) and B (0.1% TFA in CH_3CN/H_2O (60:40)), with a gradient from 30 to 60% B in 20 min (retention time was ca. 10 min). A total of five (30–50 mL) fractions were screened; three acceptable fractions were pooled and lyophilized to yield 21 (89.5 mg, 4.4%).

Synthesis and purification of 1–4 proceeded in a similar manner.

Peptide Characterization. Analytical RPHPLC. Analytical RPHPLC analysis was achieved in TEAP (pH 2.50)/acetonitrile (CH_3CN) on a Waters Associates HPLC system which was comprised of two 6000A pumps (gradient 40–70% B 30 min, at 1.5 mL/min), a Waters Associates WISP sample injector, a Vydac C_{18} column (0.46 × 25 cm, 5-μm particle size, 300-Å pore size), a Kratos Spectroflow Model 773 UV detector (at 210 nm), and a Waters Associates data module integrator/recorder or using a Hewlett-Packard apparatus composed by a Series II 1090 Liquid Chromatograph (40–70% B 30 min, at 0.2 mL/min), a Vydac C_{18} column (0.21 × 15 cm, 5-μm particle size, 300-Å pore size), a Controller 362, and a Think Jet recorder. During the preparative purification, the fractions were screened on a Waters Associates system composed of an Automated Gradient Controller, two pumps Model 510, 486 tunable absorbance detector (210 nm), a Rheodyne 7125 injector, and a Servocorder SR6253 Datamark dual-pen chart recorder (chart speed of 1 cm/min).

Capillary Zone Electrophoresis. Capillary zone electrophoresis (CZE) was done using a Beckman P/ACE System 2000 controlled by an IBM Personal System/2 Model 50Z and using a ChromJet integrator. Conditions are given in legend Table 1.

Amino Acid Analysis. Amino acid analysis of the peptides (after 4 N methanesulfonic acid hydrolysis at 110 °C for 24 h) was performed on a Perkin-Elmer LC system (Norwalk, CT) comprising of two Series 10 LC pumps, a ISS-100 sample injector, an RTC 1 column oven, a Kratos Spectroflow 980 fluorescence detector, and a LCI-100 integrator. A Pierce AA511 ion-exchange column was maintained at 60 °C and post column derivatization with *o*-phthalaldehyde was performed at 52 °C. Samples containing the internal standard γ-aminobutyric acid were injected and 5 min after injection were subjected to a gradient of 0–100% B in 25 min and then 100% B for 15 min. The flow rate was 0.5 mL/min, and A and B buffers were Pierce Pico buffer (pH 2.20) and Beckman Microcolumn sodium citrate buffer (pH 4.95), respectively. All results were consistent with expected values.

Optical Rotations. Optical rotations of peptides were measured (sodium D line) in 1% or 50% acetic acid depending on the solubility of the peptide (c = 1.0; i.e., 10 mg of lyophilized peptide/mL, uncorrected for TFA counterions or water present after lyophilization). Values were obtained from the means of 15 successive 5-s integrations determined at room temperature (~25 °C) on a Perkin-Elmer 241 polarimeter using a 100-μL cell and are quoted as uncorrected specific rotations.

Liquid Secondary Ion Mass Spectra. LSIMS mass spectra were measured with a JEOL JMS-HX110 double-focusing mass spectrometer (JEOL, Tokyo, Japan) fitted with a Cs^+ gun. An accelerating voltage of 10 kV and Cs^+ gun voltage between 25 and 30 kV were employed. The sample was added directly to a glycerol and 3-nitrobenzyl alcohol (1:1) matrix. The spectra were calibrated using $Cs(CsI)_n$ cluster peaks. The spectra were measured at a nominal resolution of either 1000, 3000, or 5000 as determined by the intact molecule ion peak intensity. For those spectra that were measured at 1000 resolution, the observed average m/z was compared with the calculated $[M + H]^+$ average mass. In those cases where the higher mass resolving power of the instrument was used (3000 or 5000), the observed m/z of the monoisotopomer was compared with the calculated $[M + H]^+$ monoisotopic mass. On the basis of the intact molecule ion isotope peak distribution intensities for the spectra measured at either 3000 or 5000 resolution, we could exclude the possibility that the disulfide bridge containing analogues contained a reduced component which amounted to more than a 5% impurity.[55] Because a large mass shift (18 Da) is characteristic of uncyclized lactam-bridged analogues, we could exclude this possibility for measurements made at both high and low resolution.

Edman Degradation. ABI Model 477A Pulsed Liquid Phase Protein Sequencer was used with ABI on line PTH amino acid analyzer. Repetitive yields were between 90 and 95%. Load of peptides was 500 pmoles.

Molecular Modeling. Molecular modeling and other computational procedures were conducted with the DISCOVER and Insight II packages (Biosym Technologies, San Diego) on a Silicon Graphics Model 310 GTX workstation using the IRIX 4.0.5 operating system. A full valence force field[49] was used to calculate potential energies. The analytical forms and parameters of this force field have been reported previously.[56]

Circular Dichroism Spectra. Circular dichroism (CD) spectra were obtained with a computer-controlled Aviv Model 62DS spectropolarimeter (Aviv Associates, Lakewood, NJ) under the control of the manufacturer's 60DS operating system. Spectra were collected at 1.0-nm intervals in the range 190–250 nm as the average of four runs using a 2.0-s integration time and a spectral band width of 2.0 nm in 0.5-mm cuvettes thermostated at 20 °C.

Spectra were collected under two sets of buffer conditions: (1) 0.02 M sodium phosphate, 0.05 M sodium chloride (pH 6.5), and (2) the same buffer diluted 1/1 (v/v) with 2,2,2-trifluoroethanol (TFE). Concentrations were based on the calculated molecular weight of the TFA salt of the purified lyophilized peptide. Residue molar elipticities were calculated based on the number of residues in each analogue, irrespective of any side chain bridging amide bonds.

Biological Testing. Rat anterior pituitary glands from male Sprague–Dawley rats were dissociated by collagenase and plated (0.16×10^6 cells/well in 48-well plates) in medium containing 2% fetal bovine serum (FBS).[47] Three days after plating, the cells were washed three times with fresh medium containing 0.1% bovine serum albumin (BSA) and incubated for 1 h. Following the 1-h preincubation, the cells were washed once more and the test peptides were applied in the absence (determination of intrinsic activity) or the presence (testing of antagonistic activity) of 1 nM oCRF. At the end of a 3-h incubation period, the media were collected and the level of ACTH was determined by radioimmunoassay (Diagnostic Products Corp.). The percent intrinsic activity of each of the antagonists is calculated by determining level of secretion caused by the highest dose of antagonist (in the absence of oCRF) minus basal secretion and dividing that number by the level of secretion of 1 nM oCRF minus basal secretion and multiplying the result by 100.

Acknowledgment. This work was supported in part by NIH Grant no. DK-26741, The Hearst Foundation, the Foundation for Research, and the Foundation for Medical Research, Inc. Drs. W. Vale, C. Rivier, and A. Craig are FR and FMR investigators. Dr. Antonio Miranda was supported by a Postdoctoral Fellowship provided by CNPq, Conselho Nacional de Desenvolvimento Científico e Tecnológico, Brazil, and his present address is Escola Paulista de Medicina, Rua 03 de Maio, 100, São Paulo, São Paulo, Brazil 04034. We thank Laura Cervini, Charleen Miller, J. Dykert, Ron Kaiser, John Porter, Duane Pantoja, Yaira Haas, and Stephanie Leonard for technical assistance and R. Hensley for manuscript preparation.

References

(1) Vale, W.; Spiess, J.; Rivier, C.; Rivier, J. Characterization of a 41 residue ovine hypothalamic peptide that stimulates the secretion of corticotropin and β-endorphin. *Science* **1981**, *213*, 1394–1397.
(2) Spiess, J.; Rivier, J.; Vale, W. Characterization of rat hypothalamic growth hormone-releasing factor. *Nature* **1983**, *303*, 532–535.
(3) Spiess, J.; Rivier, J.; Vale, W. Sequence analysis of rat hypothalamic corticotropin-releasing factor with the orthophthalaldehyde strategy. *Biochemistry* **1983**, *22*, 4341–4346.
(4) Ling, N.; Esch, F.; Bohlen, P.; Baird, A.; Guillemin, R. Isolation and characterization of caprine corticotropin-releasing factor. *Biochem. Biophys. Res. Commun.* **1984**, *122*, 1218–1224.
(5) Esch, F.; Ling, N.; Bohlen, P.; Baird, A.; Benoit, R.; Guillemin, R. Isolation and characterization of the bovine hypothalamic corticotropin-releasing factor. *Biochem. Biophys. Res. Commun.* **1984**, *122*, 899–905.
(6) Patthy, M.; Horvath, J.; Mason-Garcia, M.; Szoke, B.; Schlesinger, D. H.; Schally, A. V. Isolation and amino acid sequence of corticotropin-releasing factor from pig hypothalami. *Proc. Natl. Acad. Sci. U.S.A.* **1985**, *82*, 8762–8766.
(7) Shibahara, S.; Morimoto, Y.; Furutani, Y.; Notake, M.; Takahashi, H.; Shimizu, S.; Horikawa, S.; Numa, S. Isolation and sequence analysis of the human corticotropin-releasing factor precursor gene. *Embo J.* **1983**, *2* (5), 775–779.
(8) Furutani, Y.; Morimoto, Y.; Shibahara, S.; Noda, M.; Takahashi, H.; Hirose, T.; Asai, M.; Inayama, S.; Hayashida, H.; Miyata, T.; Numa, S. Cloning and sequence analysis of cDNA for ovine corticotorpin-releasing factor precursor. *Nature* **1983**, *301*, 537–540.
(9) Jingami, H.; Mizuno, N.; Takahashi, H.; Shibahara, S.; Furutani, Y.; Imura, H.; Numa, S. Cloning and sequence analysis of cDNA for rat corticotropin-releasing factor precursor. *FEBS Lett.* **1985**, *191*, 63–66.
(10) Thompson, R. C.; Seasholtz, A. F.; Herbert, E. Rat corticotropin-releasing hormone gene: sequence and tissue-specific expression. *Mol. Endocrinol.* **1987**, *1*, 363–370.
(11) Montecucchi, P. C.; Henschen, A. Amino acid composition and sequence analysis of sauvagine, a new active peptide from skin of *Phyllomedusa sauvagei*. *Int. J. Peptide Prot. Res.* **1981**, *18*, 113–120.
(12) Montecucchi, P. C.; Gozzini, L. Secondary structure prediction of sauvagine, a novel biologically active polypeptide from a frog. *Int. J. Peptide Prot. Res.* **1982**, *20*, 139–143.
(13) Lederis, K.; Letter, A.; McMaster, D.; Moore, G. Complete amino acid sequence of urotensin I, a hypotensive and corticotropin-releasing neuropeptide from *Catostomus*. *Science* **1982**, *218*, 162–164.
(14) Ichikawa, T.; McMaster, D.; Lederis, K.; Kobayaashi, H. Isolation and amino acid sequence of urotensin I, a vasoactive and ACTH releasing neuropeptide from the carp. *Peptides* **1982**, *3*, 859–867.
(15) Kataoka, H.; Troetscher, R. G.; Li, J. P.; Kramer, S. J.; Carney, R. L.; Schooley, D. A. Isolation and identification of a diuretic hormone from the tobacco hornworm, *Manduca sexta*. *Proc. Natl. Acad. Sci. U.S.A.* **1989**, *86*, 2976–2980.
(16) Blackbum, M. B.; Kingan, T. G.; Bodnar, W.; Shabanowitz, J.; Hunt, D. F.; Kempe, T.; Wagner, R. M.; Raina, A. K. L.; Schnee, M. E.; Ma, M. C. Isolation and identification of a new diuretic peptide from the tobacco hornworm, *Manduca sexta*. *Biochem. Biophys. Res. Commun.* **1991**, *181*, 927–932.
(17) Okawara, Y.; Morley, S. D.; Burzio, L. O.; Zwiers, H.; Lederis, K.; Richter, D. Cloning and sequence analysis of cDNA for corticotropin-releasing factor precursor from teleost fish *Catostomus commersoni*. *Proc. Natl. Acad. Sci. U.S.A.* **1988**, *85*, 8439–8443.
(18) Rivier, C.; Rivier, J.; Lederis, K.; Vale, W. *In vitro* and *in vivo* ACTH-releasing activity of ovine CRF, sauvagine and urotensin I. *Reg. Pep.* **1983**, *5*, 139–143.
(19) Rivier, C. L.; Plotsky, P. M. Mediation by corticotropin-releasing factor (CRF) of adenohypophysial hormone secretion. In *Annual Review of Physiology*; Berne, R. M., Eds.; Academic Press: Palo Alto, CA, 1986; Vol. 48, pp 475–494.
(20) Brown, M. R. Brain peptide regulation of autonomic nervous and neuroendocrine functions. In *Stress Neurobiology and Neuroendocrinology*; Brown, M. R., Koob, G. F., Rivier, C., Eds.; Marcel Dekker, Inc.: New York, 1991; pp 193–215.
(21) Koob, G. F. Behavioral responses to stress. Focus on corticotropin-releasing factor. In *Stress Neurobiology and Neuroendocrinology*; Brown, M. R., Koob, G. F., Rivier, C., Eds.; Marcel Dekker, Inc.: New York, 1991; pp 225–271.
(22) Brown, M. R.; Fisher, L. A.; Spiess, J.; Rivier, C.; Rivier, J.; Vale, W. Corticotropin-releasing factor: actions on the sympathetic nervous system and metabolism. *Endocrinology* **1982**, *111*, 928–931.
(23) Swanson, L. W.; Sawchenko, P. E.; Rivier, J.; Vale, W. W. Organization of ovine corticotropin releasing factor (CRF)-immunoactive cells and fibers in the rat brain: An immunohistochemical study. *Neuroendocrinology* **1983**, *36*, 165–186.
(24) Rivier, J.; Rivier, C.; Vale, W. Synthetic competitive antagonists of corticotropin releasing factor: Effect on ACTH secretion in the rat. *Science* **1984**, *224*, 889–891.
(25) Rivier, C.; Vale, W. Involvement of corticotropin-releasing factor and somastostatin in stress-induced inhibition of growth hormone secretion in the rat. *Endocrinology* **1985**, *117*, 2478–2482.
(26) Rivier, C.; Rivier, J.; Vale, W. Stress-induced inhibition of reproductive functions: Role of endogenous corticotropin-releasing factor. *Science* **1986**, *231*, 607–609.
(27) Krahn, D. D.; Gosnell, B. A.; Grace, M.; Levine, A. S. CRF antagonist partiallly reverses CRF- and stress-induced effects on feeding. *Brain Res. Bull.* **1986**, *17*, 285–289.
(28) Berridge, C. W.; Dunn, A. J. A corticotropin-releasing factor antagonist reverses the stress-induced changes of exploratory behavior in mice. *Horm. Behav.* **1987**, *21*, 393–401.
(29) Tazi, A.; Dantzer, R.; LeMoal, M.; Rivier, J.; Vale, W.; Koob, G. F. Corticotropin releasing factor antagonist blocks stress-induced fighting in rats. *Reg. Pep.* **1987**, *18*, 37–42.
(30) Stephens, R. L., Jr.; Yang, H.; Rivier, J.; Taché, Y. Intracisternal injection of CRF antagonist blocks surgical stress-induced inhibition of gastric secretion in the rat. *Peptides* **1988**, *9*, 1067–1070.
(31) Kalin, N.; Sherman, J.; Takahashi, L. Antagonism of endogenous CRF system attenuates stress-induced freezing behavior in rats. *Brain Res.* **1988**, *457*, 130–135.
(32) Cole, B. J.; Cador, M.; Stiunus, L.; Rivier, J.; Vale, W.; Koob, G. F.; LeMoal, M. Central administration of a CRF antagonist blocks the development of stress-induced behavioral sensitization. *Brain Res.* **1990**, *512*, 343–346.
(33) Lau, S. H.; Rivier, J.; Vale, W.; Kaiser, E. T.; Kezdy, F. J. Surface properties of an amphiphilic peptide hormone and of its analog: Corticotropin-releasing factor and sauvagine. *Proc. Natl. Acad. Sci. U.S.A.* **1983**, *80*, 7070–7074.
(34) Pallai, P. V.; Mabilia, M.; Goodman, M.; Vale, W.; Rivier, J. Structural homology of corticotropin-releasing factor, sauvagine, and urotensin I: Circular dichroism and prediction studies. *Proc. Natl. Acad. Sci. U.S.A.* **1983**, *80*, 6770–6774.
(35) Fisher, L.; Rivier, C.; Rivier, J.; Brown, M. Differential antagonist activity of α-helical CRF(9–41) in three bioassay systems. *Endocrinology* **1991**, *129*, 1312–1316.

(36) Rivier, J.; Rivier, C.; Galyean, R.; Yamamoto, G.; Vale, W. Corticotropin releasing factor: characterization of new analogs. In *Peptide Chemistry 1987*; Shiba, T., Sakakibara, S., Eds.; Protein Research Foundation, Osaka, 1988; pp 597–600.
(37) Rivier, J.; Rivier, C.; Koerber, S. C.; Kornreich, W. D.; Miranda, A.; Miller, C.; Galyean, R.; Porter, J.; Yamamoto, G.; Donaldson, C. J.; Vale, W. Structure activity relationships (SAR) of somatostatin, gonadotropin, corticotropin and growth hormone releasing factors. In *Peptides: Chemistry and Biology*; Smith, J. A., Rivier, J. E., Eds.; ESCOM Science Publishers B. V.: Leiden, The Netherlands, 1992; pp 33–36.
(38) Romier, C.; Bernassau, J.-M.; Cambillau, C.; Darbon, H. Solution structure of human corticotropin releasing factor by ^{1}H NMR and distance geometry with restrained molecular dynamics. *Prot. Eng.* **1993**, *6*, 149–156.
(39) Hernandez, J.-F.; Kornreich, W.; Rivier, C.; Miranda, A.; Yamamoto, G.; Andrews, J.; Taché, Y.; Vale, W.; Rivier, J. Synthesis and relative potencies of new constrained CRF antagonists. *J. Med. Chem.* **1993**, *36*, 2860–2867.
(40) Felix, A. M.; Heimer, E. P.; Wang, C. T.; Lambros, T. J.; Fournier, A.; Mowles, T. F.; Maines, S.; Campbell, R. M.; Wegrzynski, B. B.; Toome, V.; Fry, D.; Madison, V. S. Synthesis, biological activity and conformational analysis of cyclic GRF analogs. *Int. J. Peptide Prot. Res.* **1988**, *32*, 441–454.
(41) Cervini, L. A.; Corrigan, A.; Donaldson, C. J.; Koerber, S. C.; Vale, W. W.; Rivier, J. E. Cyclic analogs of [MeTyr^1,Ala^{15},Nle^{27}]GRF-(1–29)-NH_2 with high potencies *in vitro*. In *Peptides: Chemistry, Structure and Biology*; Hodges, R. S., Smith, J. A., Eds.; ESCOM Science Publishers B. V.: Leiden, The Netherlands, 1993; in press.
(42) Rivier, J.; Vale, W.; Burgus, R.; Ling, N.; Amoss, M.; Blackwell, R.; Guillemin, R. Synthetic luteinizing hormone releasing factor analogs. Series of short-chain amide LRF homologs converging to the amino terminus. *J. Med. Chem.* **1973**, *16*, 545–549.
(43) Castro, B.; Dormoy, J. R.; Evin, G.; Selve, C. Réactifs de couplage peptidique IV (1) - L'hexafluorophosphate de benzotriazolyl n-oxytrisdimethylamino phosphonium (B.O.P.). (Peptide coupling reagents. IV. N-[Oxytris(dimethylamino)phosphonium]benzotriazole hexafluorophosphate.) *Tetrahedron Lett.* **1975**, *14*, 1219–1222.
(44) Hoeger, C.; Galyean, R.; Boublik, J.; McClintock, R.; Rivier, J. Preparative reversed phase high performance liquid chromatography. II. Effects of buffer pH on the purification of synthetic peptides. *Biochromatography* **1987**, *2*, 134–142.
(45) Rivier, J.; Rivier, C.; Galyean, R.; Miranda, A.; Miller, C.; Craig, A. G.; Yamamoto, G.; Brown, M.; Vale, W. Single point D-substituted corticotropin releasing factor analogues: Effects on potency and physicochemical characteristics. *J. Med. Chem.* **1993**, *36*, 2851–2859.
(46) Yang, J. T.; Wu, C.-S. C.; Martinez, H. M. Calculation of protein conformation from circular dichroism. In *Methods in Enzymology*; Hirs, C. H. W., Timasheff, S. N., Eds.; Academic Press: New York, 1986; Vol. 130, pp 228.
(47) Vale, W.; Vaughan, J.; Yamamoto, G.; Bruhn, T.; Douglas, C.; Dalton, D.; Rivier, C.; Rivier, J. Assay of corticotropin releasing factor. In *Methods in Enzymology: Neuroendocrine Peptides*; Conn, P. M., Eds.; Academic Press: New York, 1983; Vol. 103, pp 565–577.
(48) Kornreich, W. D.; Galyean, R.; Hernandez, J.-F.; Craig, A. G.; Donaldson, C. J.; Yamamoto, G.; Rivier, C.; Vale, W.; Rivier, J. Alanine series of ovine corticotropin releasing factor (oCRF): a structure-activity relationship study. *J. Med. Chem.* **1992**, *35*, 1870–1876.
(49) Hagler, A. T. Theoretical simulation of conformation, energetics and dynamics of peptides. In *The Peptides: Analysis, Synthesis, Biology*; Udenfriend, S., Meienhofer, J., Hruby, V. J., Eds.; Academic Press: Orlando, FL, 1985; Vol. 7, pp 213–299.
(50) Felix, A. M.; Wang, C.-T.; Campbell, R. M.; Toome, V.; Fry, D. C.; Madison, V. S. Biologically active cyclic (lactam) analogs of growth hormone-releasing factor: Effect of ring size and location on conformation and biological activity. In *Peptides. Chemistry and Biology*; Smith, J. A., Rivier, J. E., Eds.; ESCOM Science Publishers, B. V.: Leiden, The Netherlands, 1992; pp 77–79.
(51) Shoemaker, K. R.; Kim, P. S.; York, E. J.; Stewart, J. M.; Baldwin, R. L. Tests of the helix dipole model for stabilization of α-helices. *Nature* **1987**, *326*, 563–567.
(52) Almquist, R. G.; Kadambi, S. P.; Yasuda, D. M.; Weitl, F. L.; Polgar, W. E.; Toll, L. R. Paralytic activity of (des-Glu^1)conotoxin GI analogs in the mouse diaphragm. *Int. J. Peptide Prot. Res.* **1989**, *34*, 445–462.
(53) Kaiser, E.; Colescott, R. L.; Bossinger, C. D.; Cook, P. I. Color test for detection of free terminal amino groups in the solid-phase synthesis of peptides. *Anal. Biochem.* **1970**, *34*, 595–598.
(54) Rivier, J.; McClintock, R.; Galyean, R.; Anderson, H. Reversed phase HPLC: Preparative purification of synthetic peptides. *J. Chromatog.* **1984**, *288*, 303–328.
(55) Craig, A. G.; Rivier, J. E. Metastable fragmentation of somatostatin-14 (SS-14) and a series of SS-14 analogs formed with liquid secondary ion mass spectrometry: observation of fragment ions which involve unsymmetric disulfide bridge cleavage concomitant with peptide chain cleavage. *Org. Mass. Spectrom.* **1992**, *27*, 549–559.
(56) Hagler, A. T.; Lifson, S. Energy function for peptides and proteins: I. Derivation of a consistent force field including the hydrogen bond from amide crystals. *J. Am. Chem. Soc.* **1974**, *96*, 5319–5327.